

# Order–Disorder Phase Transition in Heterogeneous Populations of Self-propelled Particles

Gil Ariel · Oren Rimer · Eshel Ben-Jacob

Received: 24 February 2014 / Accepted: 12 August 2014  
© Springer Science+Business Media New York 2014

**Abstract** Biological systems are typically heterogeneous as individuals vary in their characteristics, their response to the external environment and to each other. For example, cell diversity plays a crucial role in the successful survival of many biological systems. Phenotypic heterogeneity is associated with cellular response to intercellular communications, the response to external environmental cues, motility modes, and proliferation rates. Here we study the effect of phenotypic diversity on the properties of collective motion in the context of the scalar noise model of collective migration. For simplicity, we study a population that is composed of two sub-populations, each with different sensitivities to external noise. We find that the two sub-populations interact non-additively: Within a large range of parameters, the dynamics of the system can be described by an equivalent homogeneous system with an effective temperature that depends on the average circular mean of the phenotypes. However, if one of the sub-populations is sufficiently “cold”, it dominates the dynamics of the group as a whole.

**Keywords** Collective motion · Self propelled particles · Heterogeneous populations · Order–disorder phase transition

## 1 Introduction

Complex systems, in particular biological systems, are typically heterogeneous as individuals have disparate characteristics and vary in their properties. In some examples, variations in

---

G. Ariel (✉) · O. Rimer  
Department of Mathematics, Bar-Ilan University, 5290002 Ramat-Gan, Israel  
e-mail: arielg@math.biu.ac.il

E. Ben-Jacob  
School of Physics and Astronomy, Tel-Aviv University, 69978 Tel-Aviv, Israel

E. Ben-Jacob  
Biological Physics, Rice University, Houston, TX 77005, USA  
e-mail: eshelbj@gmail.com

properties average out and do not have any significant effect on the macroscopic properties of the system. However, in many other cases diversity can have a pivotal effect on the system dynamics. For example, it was shown that size variation in excited granular material can lead the system to separate according to size. The impact of heterogeneity on the properties of collective motion, in particular on the order–disorder phase transition, has not been thoroughly studied. Within the context of simplified models of self-propelled particles addressing the general and broad description of the dynamics, most models focus on homogeneous system. That is, it is assumed that all the agents have the same properties and follow the same “rules of engagement” [1]. Notable exceptions are introduction of leaders [2] which creates an expected bias towards the leading population, variability in speed [3], which was found to only affect the rate of convergence to a stationary distribution but not the distribution itself, and variable interactions between two sub-populations [4].

In this paper, we study the effect of heterogeneity in the context of the well-studied scalar noise model (SNM), proposed by Viscsek et. al. [5, 6]. In this model,  $N$  particles move with constant speed  $v$  in a rectangular two-dimensional domain  $[0, L]^2$  with periodic boundary conditions. Every simulation time step, each particle aligns its direction with the average direction of all particles within an interaction distance  $R$  and makes a random turn. In [6], the random turn is taken to be uniformly distributed in a fixed range  $[-\eta, \eta]$  for some fixed  $\eta \in [0, \pi]$ . It is shown numerically that the system undergoes a phase transition between an ordered phase at low temperature/high density and a disordered phase at high temperature/low density. Various aspects of the transition have been studied in the rapidly expanding literature on the SNM and its many variants. For recent reviews see [1, 7].

Phase transitions are typically characterized by the scaling of an order parameter - the norm of the average velocity in the case of SNM - close to a critical density  $\rho = N/L^2$  or critical temperature. As density is an extensive global parameter, it cannot be directly related to the properties of individuals. On the other hand, temperature is clearly related to, loosely speaking, the “amount of noise in the system”, which is characterized by  $\eta$  - a property of individuals. This motivates us to examine a mixed population of particles, each with a different noise parameter. For simplicity, we consider a binary mixture, in which a fraction  $f_1$  of the particles have noise  $U(-\eta_1, \eta_1)$ , while a fraction  $f_2 = 1 - f_1$  have noise  $U(-\eta_2, \eta_2)$ , where  $U(a, b)$  denoted the uniform distribution in  $(a, b)$ .

The layout of the paper is as follows. Section 2 details the model and discusses the notion of temperature in the context of SVM. We found that it is essential to select the proper measures associated with the statistics of the order parameter for comparing the behaviors of homogeneous populations vs. heterogeneous ones, Sect. 3 presents our main results. In particular, we demonstrate numerically that parameter variability has a non-additive effect which *promotes order* in the sense that a heterogeneous population can be in the ordered phase while a homogeneous one with the same temperature is disordered. We conclude in Sect. 4.

## 2 The Scalar Noise Model

Consider  $N$  particles moving in a rectangular two-dimensional domain  $[0, L]^2 \subset \mathbb{R}^2$  with fixed speed  $v$ . Let  $x_i^k$  denote the position of particle  $i$  at time  $k$  and  $\hat{h}_i^k$ , the normalized “head direction”,  $|\hat{h}_i^k| = 1$ . For convenience, we denote the angle between  $\hat{h}_i^k$  and the x-axis  $\theta_i^k$ ,  $\hat{h}_i^k = (\cos \theta_i^k, \sin \theta_i^k)$ . The  $N$  particles are divided into two sub-species: Particles  $1 \dots N_1$  are species 1, while particles  $N_1 + 1 \dots N$  are species 2. Let  $p_i$  denote the species index of

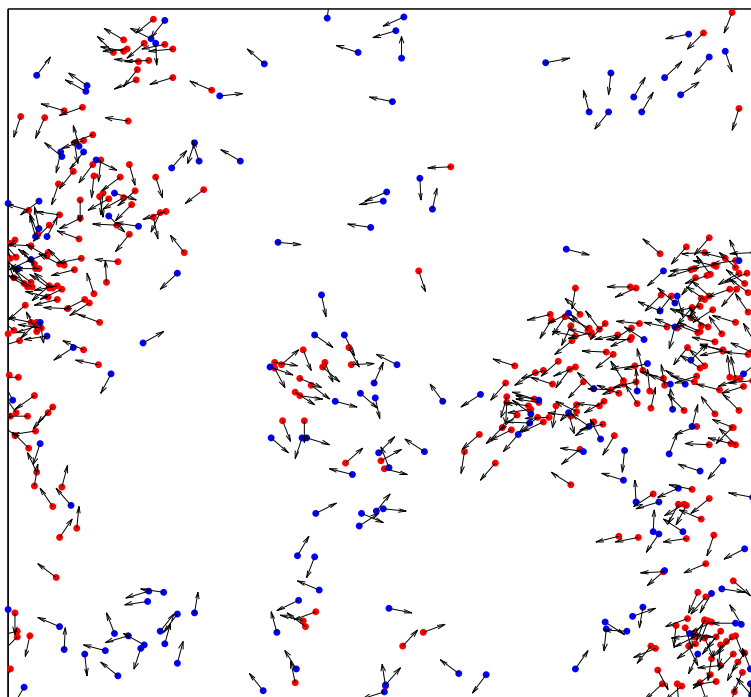


**Fig. 1** A snapshot from a simulation with 500 particles (Color figure online)

particle  $i$ ,  $p_i = 1$  for  $i = 1, \dots, N_1$  and  $p_i = 2$  otherwise. We consider a discrete dynamical system which evolves according to the following rules (performed synchronously and in order)

1. Advance:  $x_i^{k+1} = x_i^k + v\hat{h}_i^k$ .
2. Align:

$$\tilde{h}_i^{k+1} = \frac{1}{n_i^k} \sum_{j \in A_i^k} \hat{h}_j, \quad (2.1)$$

where  $A_i^k = \{j : |x_i^k - x_j^k| \leq R\}$ , the set of neighbors of  $i$  at time  $k$  within an interaction distance  $R$  and  $n_i^k = |A_i^k|$  is the number of neighbors.

3. Random turn: Rotate  $\tilde{h}_i^{k+1}$  by a random angle and normalize. Specifically, let  $\alpha_i^k$  denote a random angle, uniformly distributed in  $[-\eta_{p_i}, \eta_{p_i}]$ ,  $\alpha_i^k \sim U(-\eta_{p_i}, \eta_{p_i})$ . Then,  $\hat{h}_i^{k+1} = \tilde{h}_i^{k+1} / |\tilde{h}_i^{k+1}|$ , where

$$h_i^{k+1} = \begin{pmatrix} \cos \alpha_i & -\sin \alpha_i \\ \sin \alpha_i & \cos \alpha_i \end{pmatrix} \tilde{h}_i^{k+1}. \quad (2.2)$$

With  $\eta_1 = \eta_2$ , the model reduces to the standard SNM described in [6]. Figure 1 shows a snapshot from a simulation with 500 particles. Parameters are  $f_1 = 2/3$ ,  $f_2 = 1/3$ ,  $\eta_1 = \pi/3$ ,  $\eta_2 = 2\pi/3$ ,  $R = 1$ ,  $\rho = 2$  and  $v = 0.1$ .

With random initial conditions (uniform spatial distribution and uniform angles), the system relaxes into a steady state that can be characterized by an order parameter, which is the norm of the average head direction

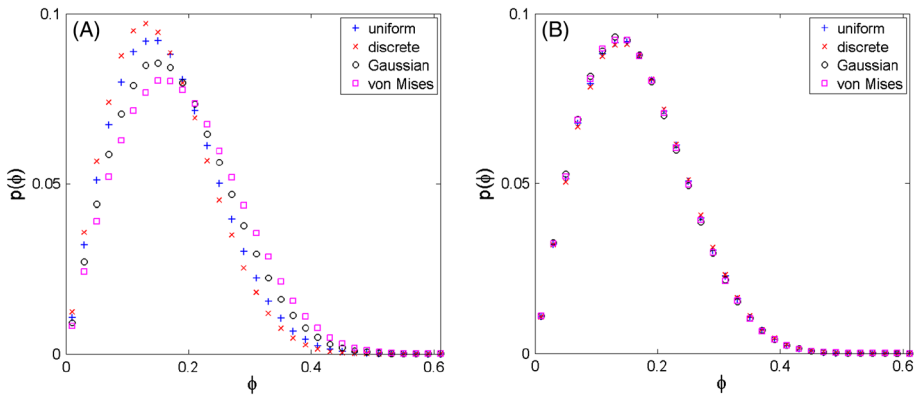


**Fig. 2** The distribution of  $\phi$  with different choices of noise. **a** All noise distributions have the same variance. **b** All noise distributions have the same circular mean (Color figure online)

$$\phi^k = \left| \frac{1}{N} \sum_j \hat{h}_j^k \right|. \quad (2.3)$$

We will also be interested in the average order parameter  $\phi = \langle \phi^k \rangle$ , where  $\langle \cdot \rangle$  denotes averaging with respect to all time steps, all particles and possibly repeated simulations.

The choice of uniformly distributed random turns seems arbitrary. Indeed, other choices have been used in the literature such as Gaussian or the von Mises distribution [8–11]. The latter is the maximum entropy distribution for a given circular mean, and is described by the probability density  $p(\alpha) = \exp(\kappa \cos(\alpha - \mu)) / (2\pi I_0(\kappa))$ , where  $I_0(z)$  is the zero'th order modified Bessel functions of the first kind. The parameter  $\mu$  is the average angle and  $1/\kappa$  is related to the variance. Figure 2a shows the distribution of  $\phi^k$  obtained for a homogeneous population ( $\eta_1 = \eta_2 = \eta$ ) with four different choices of distributions for the random turning angles: uniform distribution, Gaussian, Bernoulli ( $\pm\eta$  with equal probability) and von Mises (with  $\mu = 0$ ). Parameters were chosen so that all distributions have the same variance. Clearly, the steady state depends on the choice of noise. Instead, one should consider circular statistics [10]. Let  $\alpha$  denote a real random variable. The circular mean of  $\alpha$  is defined as

$$\mathbb{E}[e^{i\alpha}] = \mathbb{E}[\cos \alpha] + i \mathbb{E}[\sin \alpha]. \quad (2.4)$$

To resolve the issue studied here (homogeneous vs. heterogeneous populations), we focused on distributions that have even densities, hence, the imaginary part vanishes. For example, with a uniform distribution  $\alpha \sim U[-\eta, \eta]$ , we have that

$$\mathbb{E}[e^{i\alpha}] = \int_{-\eta}^{\eta} p(\alpha) e^{i\alpha} d\alpha = \int_{-\eta}^{\eta} \frac{1}{2\eta} (\cos \alpha + i \sin \alpha) d\alpha = \text{sinc}(\eta).$$

Indeed, Fig. 2B shows the distribution of  $\phi$  for the same four distributions with parameters chosen such that all distributions have the same circular mean. The steady states are equivalent up to statistical error. To this end, we use the circular average to define the temperature as follows

$$\begin{aligned} T_1 &= 1 - \text{sinc}(\eta_1) \\ T_2 &= 1 - \text{sinc}(\eta_2) \\ T &= f_1 T_1 + f_2 T_2. \end{aligned} \quad (2.5)$$

We note that  $T$  is in  $[0, 1]$  and is increasing with increasing noise. The circular mean is also related to the average order parameter. Denote

$$\beta_i^k = \theta_i^{k+1} - \theta_i^k. \quad (2.6)$$

In words,  $\beta_i^k$  is the change in direction particle  $i$  makes following step  $k$ , including both alignment and random turning. Therefore,  $\cos \beta_i^k$  is the projection of the new direction on the previous one. In particular, suppose the system is perfectly aligned,  $\phi^k = 1$ . After a single step  $\phi^{k+1} = (1/N) \sum_j \cos \beta_j^k$ , i.e., the average turn. Hence,  $\phi = \langle \cos \beta_i^k \rangle$  is the observed circular mean. This identity is confirmed in simulations, see also [12]. The difference between the observed circular mean  $\phi = \langle \cos \beta_i^k \rangle$  and the circular mean of the random turns is always negative since alignment decreases the spread of angles.

### 3 Results

The main objective of the paper is a systematic comparison between the physical properties of homogeneous systems ( $T_1 = T_2 = T$ ) and heterogeneous ones ( $T_1 \neq T_2$ ), having the same overall temperature  $T$ . In particular, we are interested in finding the effect of heterogeneity on the critical temperature at fixed concentrations.

Numerically, one of the most precise methods for detecting the critical temperatures is by comparing the Binder cumulant at different temperatures and concentrations [11–13]. However, with heterogeneous populations such a comparison is not trivial since, due to finite size fluctuations, the location of the critical point may not be the same along different cuts in the  $T_1 - T_2$  plane. For this reason, we will consider a different measure that qualitatively distinguishes between ordered and disordered systems. Consider the location of the maximum in the distributions (the mode) of the order parameter described in Fig. 3. With a low

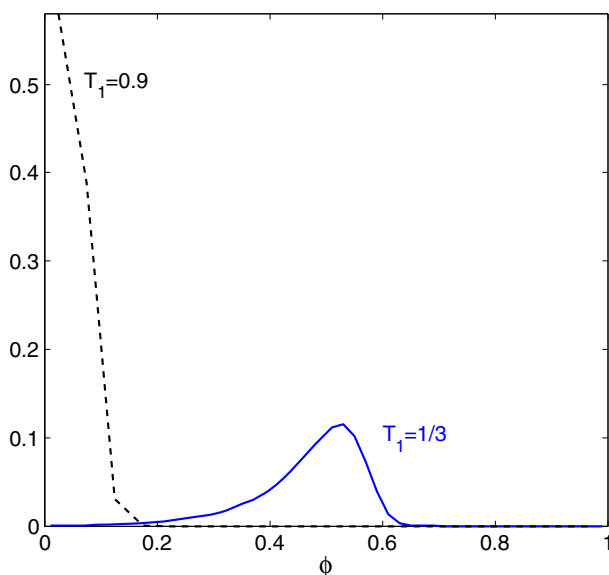


**Fig. 3** The steady state distribution of the order parameter  $\phi$ .  $T_2 = 2/3$  (Color figure online)

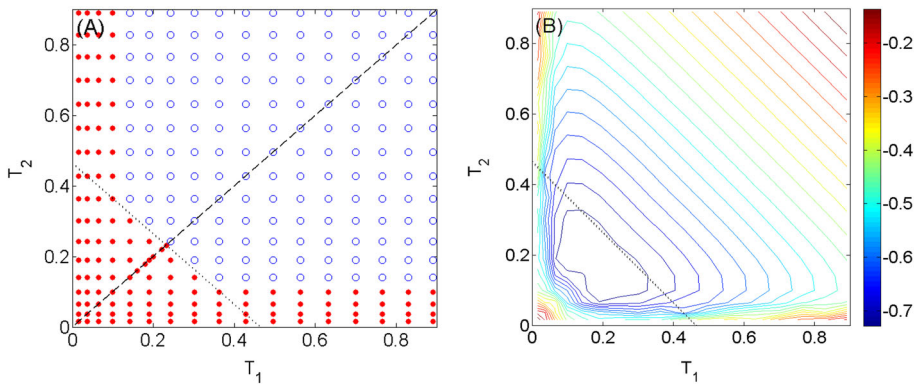


**Fig. 4** A heterogeneous system with 50,000 particles at  $f_1 = f_2 = 1/2$ . **a** The phase diagram. Red dots indicate an ordered phase, while blue circles are disordered. **b** The difference between the observed circular mean  $\phi$  and the circular mean of the random turns  $1 - T$ . Up to statistical error, if  $T_1$  or  $T_2$  are small enough, level curves are close to horizontal or vertical lines. Otherwise, they are diagonal lines, indicating a constant temperature. The dashed curve shows the homogeneous  $T_1 = T_2$  line. The dotted line is the constant temperature curve passing through the homogeneous critical temperature (Color figure online)

temperature (solid blue curve), the mode is around  $\phi = 0.5$ . However, when the temperature is high enough (dashed black curve), the density is monotonically decreasing and the mode is at  $\phi = 0$ . A non-monotone density is typically associated with increased kurtosis, which is, up to a constant, the Binder cumulant. Accordingly, we will refer to the case in which the mode is strictly positive (more precisely, larger than  $2/\sqrt{N}$ ) as the ordered phase. Otherwise, we will refer to it as disordered.

Figure 4a shows the phase diagram of a symmetrically mixed population ( $f_1 = f_2 = 1/2$ ) as a function of  $T_1$  and  $T_2$ . Red points indicate a system in the ordered phase (mode  $> 0$ ) while blue points indicate a disordered phase. The dashed diagonal line is the homogeneous  $T_1 = T_2$  case. As a reference, Fig. 5 shows the phase diagram of the same 2-population mixtures when the two populations are not interacting. In this simple case, the system is in the ordered phase only if both sub-populations are ordered. However, when the two populations are interacting, it is evident that heterogeneity has a non-trivial effect on the steady state. In particular, if one of the species is “cold enough” (either  $T_1$  or  $T_2$  are below approximately 0.25), then the system is ordered. Note that this does not correspond to the critical temperature of a single species on its own, which is slightly higher (0.33). At intermediate temperatures the ordered–disordered transition occurs close to the dotted line which indicates the  $f_1 T_1 + f_2 T_2 = T_{\text{critical}} = 0.36$  curve. Figure 4b shows the level curves of

$$\psi(T_1, T_2) = \phi(T_1, T_2) - T - 1 = \langle \cos \beta_i^k \rangle - \langle \cos \alpha_i^k \rangle. \quad (3.1)$$

Recall that the first is the real part of the circular mean of turns as observed in simulations, i.e., including both random turns and orientation interaction. The second term is the real part of the circular mean of random turns alone. As discussed above,  $\psi$  is always negative. Similar to the phase diagram, if either  $T_1$  or  $T_2$  are sufficiently small, then the level curves of  $\psi$  are close to horizontal or vertical lines, indicating that the colder population dominates. Otherwise, the level curves have slope -1, which implies that  $\psi$  is constant at constant temperature  $T = (T_1 + T_2)/2$ . Similar behavior can be observed in Fig. 6 with  $f_1 = 3/4$ , showing an expected bias towards the first population. Simulation parameters are  $N = 50000$ ,  $v = 0.1$ ,  $R = 1$ ,  $\rho = 0.6$ . Every point in Figs. 4, 5 and 6 was obtained by averaging ten simulations,

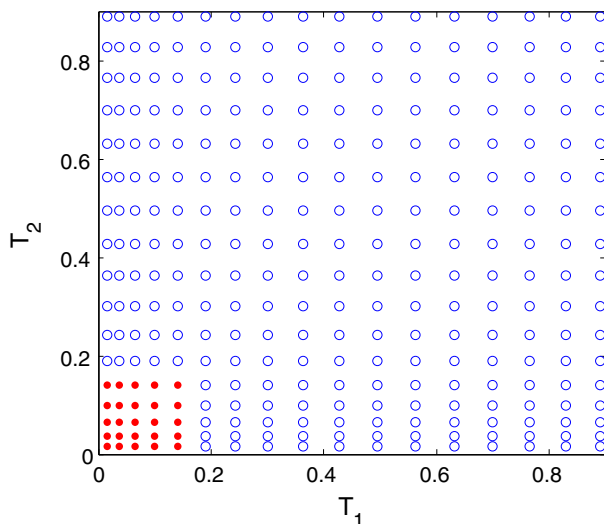


**Fig. 5** The phase diagram with a mixture of non-interacting systems. All parameters are the same as in Fig. 4. The system is in the ordered phase only if both populations are sufficiently cold (Color figure online)

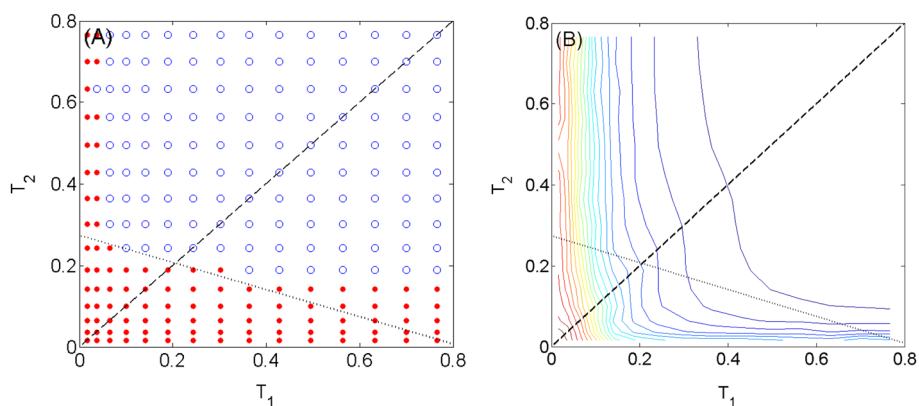


**Fig. 6** A heterogeneous system with 50,000 particles at  $f_1 = 3/4$ ,  $f_2 = 1/4$ . **a** The phase diagram. Red dots indicate an ordered phase, while blue circles are disordered. At intermediate temperatures, the transition is close to a line with slope  $-1/4$  passing through  $T_1 = T_2 = T_{\text{critical}}$ , the critical temperature of a homogeneous system. **b** The difference between the observed circular mean  $\phi$  and the circular mean of the random turns  $1 - T$ . Up to statistical error, if  $T_1$  or  $T_2$  are small enough, level curves are close to horizontal or vertical lines. The dashed curve shows the homogeneous  $T_1 = T_2$  line. The dotted line is the constant temperature curve passing through the homogeneous critical temperature (Color figure online)

each consisting of  $10^5$  steps. Simulations with a larger  $N$  did not change these observations (up to statistical errors). However, the critical temperature does weakly depend on  $N$ .

The spatial distribution of particles can be observed by analyzing the radial distribution function of each of the species, See Fig. 7. Simulation parameters are the same as in Fig. 2. Surprisingly, we find that on average, heterogeneous systems are slightly less clustered and more dispersed.

**Fig. 7** Radial distribution functions. Solid curves show the heterogeneous case: between a test particle and all other particles (*red*), between a test particle of species 1 and all other species 1 particles (*blue*), between a test particle of species 2 and all other species 2 particles (*green*) and between a test particle and all other particles belonging to the other species (*purple*). The *dashed* curve shows the radial distribution function of a homogeneous system with the same temperature (Color figure online)

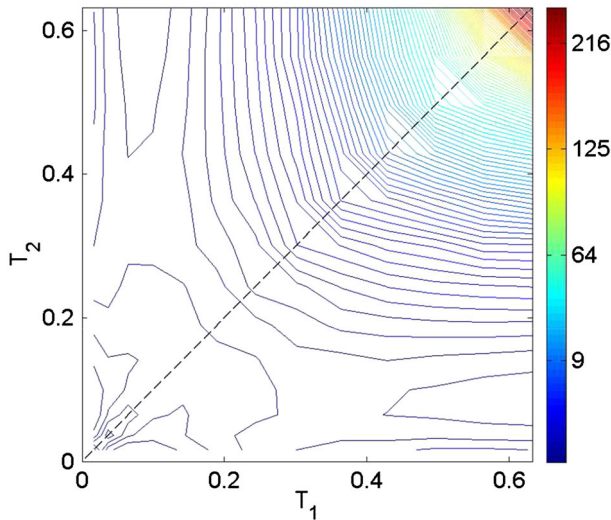
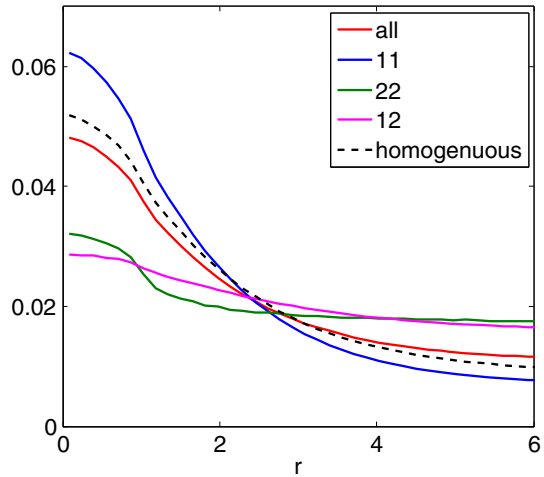


**Fig. 8** The characteristic convergence time to the steady state (Color figure online)

Finally, the rate of convergence to the steady state also depends non-trivially on parameter variability. Figure 8 shows the level curves of the characteristic convergence time as a function of  $T_1$  and  $T_2$ . Simulation parameters are  $N = 100$ ,  $f_1 = f_2 = 1/2$ ,  $v = 0.1$ ,  $R = 1$  and  $\rho = 0.3$ . Each point in Fig. 8 consists of 50,000 simulations with different number of steps. At each simulation length, the empirical distribution of  $\phi$  was evaluated until it became approximately stationary. The  $L_2$  distance between the distribution of  $\phi$  after a fixed number of steps and the steady state decay exponentially. Convergence rates were obtained by a linear least squares fit to a semi-log plot (not shown).

To further quantify the interaction between the two populations we examine the dynamics of one population in the effective mean field of the second as follows. First, we simulate a small system and estimate the average order parameter of each population,



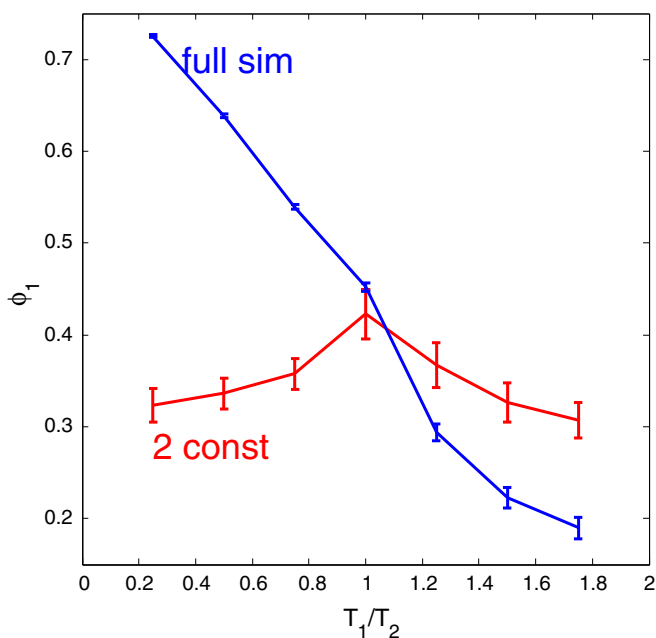


**Fig. 9** The dynamics of one population in the presence of an effective second population as a function of  $T_1/T_2$ . The curve denoted ‘full sim’ is the full simulation of the SVM described in Sect. 2. The curve denoted ‘2 const’ was generated by holding the head direction of the second population fixed with circular variance  $\phi_2$  obtained by the full simulation. Error bars show the standard deviation (Color figure online)

$$\phi_i = \left\langle \frac{1}{N_i} \sum_{p(j)=i} \hat{h}_j^k \right\rangle, \quad i = 1, 2 \quad (3.2)$$

Next, we repeat the simulation, holding the head directions of population 2 fixed. Initial conditions of population 2 are such that the circular mean of all species 2 particles is  $\phi_2$  as found in the full simulation. In other words, we fix population 2 to have the effective circular mean observed in the full simulation, including both orientation interactions and noise, and study its effect on population 1. The difference is the absence of feedback as species 2 does not respond to the dynamics of species 1. Figure 9 shows the average of  $\phi_1$  as a function of  $T_1/T_2$ . When  $T_1 = T_2$ , the interaction of population 1 with the fixed population 2 yields the same average as the full simulation. However, if  $T_1$  is different than  $T_2$ , then the two populations interact in a non-trivial manner, which cannot be described with a mean-field theory. Simulation parameters are  $N = 500$ ,  $R = 1$ ,  $v = 0.05$ ,  $\rho = 0.2$ ,  $T_2 = 0.2$  and  $f_1 = f_2 = 0.5$ . Averages were obtained by running 2,000 simulations, each with  $10^5$  steps.

## 4 Conclusion

Phenotypic heterogeneity plays an important role in cooperative survival strategies, as it renders the population more adaptable to a wide range of environmental conditions. In this paper, we demonstrated that variability in the movement characteristics among individuals can lead to macroscopic effects in groups of moving individuals. It is expected that leaders [2],

experts [14], or individualists [15], can naturally push the system towards a more ordered state. However, our results show that simply by allowing particles to have different characteristics can lead to a collective effect and induce collective motion. Intuitively, once one of the populations is cold enough to cluster and form some collective motion on its own, the other, noisier population can aggregate around areas of coordinated motion. By observing the radial distribution functions, Fig. 7, we see that with a mixed population the range of correlations between the two species is longer than in homogeneous systems. This, in turn, increases the overall consensus and synchronization in the system.

**Acknowledgments** We thank two anonymous referees for useful comments and suggestions. GA acknowledges a Marie-Curie integration grant. EBJ was supported by a grant from the Tauber Family Funds and the Maguy-Glass Chair in Physics of Complex Systems and by the NSF Center for Theoretical Biological Physics, Grant No. PHY-1308264.

## References

1. Vicsek, T., Zafeiris, A.: Collective motion. *Phys. Rep.* **517**, 71–140 (2012)
2. Couzin, I.D., Krause, J., Franks, N.R., Levin, S.A.: Effective leadership and decision-making in animal groups on the move. *Nature* **433**, 513–516 (2005)
3. Mishra, S., Tunström, K., Couzin, I.D., Huepe, C.: Collective dynamics of self-propelled particles with variable speed. *Phys. Rev. E* **86**, 011901 (Jul 2012)
4. Menzel, A.M.: Collective motion of binary self-propelled particle mixtures. *Phys. Rev. E* **85**, 021912 (2012)
5. Nagy, M., Daruka, I., Vicsek, T.: New aspects of the continuous phase transition in the scalar noise model (snm) of collective motion. *Physica A* **373**, 445–454 (2007)
6. Vicsek, T., Czirók, A., Ben-Jacob, E., Cohen, I., Shochet, O.: Novel type of phase transition in a system of self-driven particles. *Phys. Rev. Lett.* **75**, 1226–1229 (Aug 1995)
7. Toner, J., Tu, Y., Ramaswamy, S.: Hydrodynamics and phases of flocks. *Ann. Phys.* **318**(1), 170–244 (2005)
8. Degond, P., Liu, J.-G., Motsch, S., Panferov, V.: Hydrodynamic models of self-organized dynamics: derivation and existence theory. *Methods Appl. Anal.* **20**, 89–114 (2013)
9. Degond, P., Motsch, S.: Continuum limit of self-driven particles with orientation interaction. *Math. Models Methods Appl. Sci.* **18**, 1193–1215 (2008)
10. Fisher, N.I.: *Statistical Analysis of Circular Data*. Cambridge University Press, New York (1993)
11. Grégoire, G., Chaté, H., Tu, Y.: Moving and staying together without a leader. *Physica D* **181**(3), 157–170 (2003)
12. Grégoire, G., Chaté, H.: Onset of collective and cohesive motion. *Phys. Rev. Lett.* **92**, 025702 (2004)
13. Binder, K.: Finite size scaling analysis of ising model block distribution functions. *Zeitschrift für Physik B Condensed Matter* **43**(2), 119–140 (1981)
14. Cesa-Bianchi, N., Freund, Y., Haussler, D., Helmbold, D.P., Schapire, R.E., Warmuth, M.K.: How to use expert advice. *Journal of the ACM (JACM)*, **44**(3), 427–485 1997.
15. Baglietto, G., Albano, E.V., Candia, J.: Gregarious vs individualistic behavior in vicsek swarms and the onset of first-order phase transitions. *Statist. Mech. Appl. Physica A* **392**(15), 3240–3247 (2013)